[15] Odar, F., "Unsteady Motion of a Sphere Along a Circular Path in a Viscous Fluid," *Transactions of the American Society of Mechanical Engineers, Ser. E: Journal of Applied Mechanics*, Vol. 35, No. 4, Dec. 1968, pp. 652–654.

[16] Lamb, H., *Hydrodynamics*, 6th ed., Dover, New York, 1945, p. 124.

[17] Schlichting, H., *Boundary Layer Theory*, 4th ed., McGraw-Hill, New York, 1960, p. 218.

[18] Goldstein, S., ed., *Modern Developments in Fluid Dynamics*, Vol. 1, Dover, New York, 1965, pp. 181–187.

[19] Rimon, Y. and Cheng, S. I., "Numerical Solution of a Uniform Flow over a Sphere at Intermediate Reynolds Numbers," *The Physics of Fluids*, Vol. 12, No. 5, May 1969, pp. 949–959.

[20] Schmidt, F. S., "Zur beschleunigten Bewegung Kügelformig Körper in Widerstehenden Mitteln," *Annalen der Physik*, Vol. 61, No. 7, April 15, 1920, p. 633.

[21] Sarpkaya, T., "Separated Flow about Lifting Bodies and Impulsive Flow about Cylinders," *AIAA Journal*, Vol. 4, No. 3, March 1966, pp. 414–420.

[22] Lunnon, R. G., "Fluid Resistance to Moving Spheres," *Proceedings of the Royal Society*, Ser. A, Vol. 110, Feb. 1, 1926, pp. 302–326.

[23] Willmarth, W. W., Hawk, N. E., and Harvey, R. L., "Investigations of the Steady and Unsteady Motion of Freely Falling Disks," Rept. ARL 63-176, Oct. 1963, Aerospace Research Labs., Office of Aerospace Research, U.S. Air Force. (This report, with an abridged set of data tables, appeared under a similar title in *The Physics of Fluids*, Vol. 7, No. 2, Feb. 1964, pp. 197–208.)

[24] Simmons, L. F. G. and Dewey, N. S., "Wind Tunnel Experiments with Circular Disks," Repts. and Memo 1334, Feb. 1930, Aeronautical Research Council, England.

[25] Michael, P., "Steady Motion of a Disk in a Viscous Fluid," *The Physics of Fluids*, Vol. 9, No. 3, March 1966, pp. 466–471.

[26] Rimon, Y., "Numerical Solution of the Incompressible Time-Dependent Viscous Flow Past a Thin Oblate Spheroid," Rept. 2955, Jan. 1969, Naval Ship Research and Development Center, Washington, D. C.

[27] Hoerner, S. F., *Fluid-Dynamic Drag*, 1st ed., published by the author, Midland Park, N. J., 1958, pp. 3–15, 3–16.

[28] Fidleris, V. and Whitmore, R. L., "Experimental Determination of the Wall Effect for Spheres Falling Axially in Cylindrical Vessels," *British Journal of Applied Physics*, Vol. 12, Sept. 1961, pp. 490–494.

[29] Möller, W., "Experimentelle Untersuchungen zur Hydrodynamik der Kugel," *Physikalische Zeitschrift*, Vol. 39, No. 2, Jan. 15, 1938, pp. 57–80.

[30] Maskell, E. C., "A Theory of the Blockage Effects on Bluff Bodies and Stalled Wings in a Closed Wind Tunnel," Repts. and Memo 3400, Nov. 1963, Aeronautical Research Council, England.

FEBRUARY 1971 AIAA JOURNAL VOL. 9, NO. 2

Method-of-Characteristics Solution of Rarefied, Monatomic Gaseous Jet Expansion into a Vacuum

S. J. ROBERTSON*
Lockheed Missiles & Space Company, Huntsville, Ala.

AND

D. R. WILLIS†
University of California, Berkeley, Calif.

An analytical investigation was made of rarefied gas flow in an axisymmetric jet exhausting into a vacuum. A set of partial differential equations was derived for a single-component, monatomic gas by taking moments of the Boltzmann equation with the BGK approximation of the collision integral. The truncation of the moment equations was based on the hypersonic approximation. The resulting partial differential equations were solved numerically by the method of characteristics. The accuracy of the analytical technique was verified by making calculations for a spherical source flow expansion and comparing the results with those obtained by a previous investigation. The technique was then applied to the calculation of uniform parallel flow from a Mach 3.0 nozzle exhausting into a vacuum with throat Reynolds numbers of 25 and 100. Noncontinuum effects were found to have little influence on the density and velocity fields for nozzles of throat Reynolds numbers down to at least 25. The temperatures were found to behave in much the same fashion as previously predicted for spherical source flow; i.e., the parallel temperature component approaches a finite "freezing" temperature, and the two perpendicular components continue toward zero.

Nomenclature

A = constant in Eq. (2)
b = distance normal to streamline and axial plane (binormal)
f = distribution function
F = equilibrium distribution function
m = molecular mass
M = Mach number
n = distance normal to streamline in axial plane, also number density
p = pressure = $(p_s + p_n + p_b)/3$; with s,n,b or t subscript, component of pressure or shear stress as indicated by subscript
Q = factor in moment of Boltzmann equation
r = radial distance from nozzle axis, also distance from point source
r^* = sonic radius
R = nozzle exit radius
R_g = gas constant
Re^* = throat Reynolds number
s = distance along streamline

Received February 13, 1970; revision received July 2, 1970. This work was supported by NASA-Marshall Space Flight Center, Contract NAS8-21490.

* Research Specialist, Aeromechanics Department.

† Associate Professor of Aeronautical Sciences. Member AIAA.

T = temperature = $(T_s + T_n + T_b)/3$; with s,n, or b subscript, component of temperature defined by $T_s = p_s/R_g\rho$, etc.
u = mass velocity
x = axial distance measured from the nozzle exit
ζ = distance along characteristic line
η = viscosity
θ = inclination of streamline
μ = characteristic angle
ξ = molecular velocity; with subscript, component in direction indicated by subscript
ρ = mass density = mn
τ = $\tan\mu$

Subscripts

s,n or b = components corresponding to s,n or b directions
l = shear stress
o = source or chamber conditions
∞ = conditions immediately upstream of sharp corner turn

Introduction

FLOWFIELD definition of gaseous jets exhausting into a vacuum has been of increasing interest in recent years due to the use on space vehicles of small reaction motors in attitude control and maneuvering, and due to the practice of purging or venting unused propellants or liquid wastes from space vehicles into the surrounding space environment. The resulting jet plumes may impinge on surrounding vehicle surfaces, thus causing heating and pressure loads and surface contamination.

Gaseous jets exhausting into a vacuum expand to such low densities that the intermolecular collision processes are unable to sustain thermodynamic equilibrium. Therefore, the various temperatures associated with internal energy states tend to freeze at some limiting finite value rather than proceeding toward zero as in the equilibrium case. This effect has been investigated analytically by Hamel and Willis[1] and Edwards and Cheng[2] for a monatomic gas in spherical flow from a point source. The authors of Ref. 1 extended their studies to include polyatomic gases and gas mixtures in Ref. 3. References 1 and 2 employ similar approaches which involve moments of the Boltzmann equation with a solution based on matched inner and outer asymptotic expansions. The assumption is made that the nonequilibrium effects do not become significant until the flow is hypersonic. Both Refs. 1 and 2 develop equations for predicting a freezing static temperature and a corresponding limiting Mach number.

Edwards and Rogers[4] developed flowfield equations for an axisymmetric monatomic gaseous jet in hypersonic rarefied flow. These equations were developed by taking moments of the Boltzmann equation with the BGK approximation. The velocity was assumed constant at the thermodynamic limit. Although an actual solution to these equations was not attempted, it was concluded, based on inspection of the equations, that for high Reynolds number jets, the far-field rarefied solution is quite similar to the isentropic (continuum) solution.

Peracchio[5] performed a kinetic theory analysis for a two-dimensional nozzle exhausting into a vacuum. His analysis differed from the previous investigations primarily in that the solution involved the BGK equation itself rather than BGK moment equations. Peracchio emphasized in his analysis the flow in the vicinity of the corner expansion and the free streamline. No attention was given to far-field temperature freezing or to the directionalizing of random motion along streamlines.

Analytical Development

The analytical development is described as follows. A more detailed account is given in Ref. 6.

Flow Equations

The Boltzmann equation in axisymmetric streamline-normal (intrinsic) coordinates is

$$\left\{\xi_s\frac{\partial}{\partial s}+\xi_n\frac{\partial}{\partial n}+\left[\xi_n\left(\xi_s\frac{\partial\theta}{\partial s}+\xi_n\frac{\partial\theta}{\partial n}\right)+\xi_b{}^2\frac{\sin\theta}{r}\right]\frac{\partial}{\partial\xi_s}-\left[\xi_s\left(\xi_s\frac{\partial\theta}{\partial s}+\xi_n\frac{\partial\theta}{\partial n}\right)-\xi_b{}^2\frac{\cos\theta}{r}\right]\frac{\partial}{\partial\xi_n}-\xi_b\frac{\xi_s\sin\theta+\xi_n\cos\theta}{r}\frac{\partial}{\partial\xi_b}\right\}f=\left(\frac{\delta f}{\delta t}\right)_{\text{collisions}}\quad(1)$$

where $f(s,n,\xi_s,\xi_n,\xi_b)$ is the distribution function of molecular velocities; s, n and b are, respectively, the positional coordinates along the streamlines, normal to both the streamline and the axial plane, and normal to the streamline in the axial plane; ξ_s,ξ_n and ξ_b are the molecular velocities in the s, n and b directions; θ is the inclination of the streamline relative to the axis; r is the radial distance from the axis; and $(\delta f/\delta t)_{\text{collisions}}$ is time rate of change of f due to intermolecular collisions.

Flowfield equations in terms of certain physically meaningful moments of the distribution function are obtained by taking moments of the Boltzmann equation. This is accomplished by multiplying Eq. (1) by some factor, $Q(\xi_s,\xi_n,\xi_b)$; and integrating over all velocities. The following moments of the distribution function will be considered as the variables describing the flowfield.

$$\rho = m\int\int f d^3\xi,\ u = m/\rho\int\int\xi_s f d^3\xi$$
$$p_s = m\int\int(\xi_s - u)^2 f d^3\xi,\ p_n = m\int\int\xi_n{}^2 f d^3\xi$$
$$p_b = m\int\int\xi_b{}^2 f d^3\xi,\ p_t = m\int\int(\xi_s - u)\xi_n f d^3\xi$$

For moments where Q is a collision invariant, i.e., molecular mass m; linear momentum $m\xi_s$, $m\xi_n$, or $m\xi_b$; or energy $(m/2)(\xi_s{}^2 + \xi_n{}^2 + \xi_b{}^2)$; the integral of the collision term $(\delta f/\delta t)_{\text{collisions}}$, is equal to zero regardless of its form. For general Q, some simplifying assumption regarding the form of the collision term must be made in order to evaluate the integral in algebraic terms.

Edwards and Rogers[4] employed the BGK approximation[7] to the collision term

$$(\delta f/\delta t)_{\text{collisions}} = An(F - f)\quad(2)$$

where A is a constant, n is the number density (molecules per unit volume), and F is the equilibrium distribution function. Edwards and Rogers derived their equations letting the value of A remain unspecified. The BGK approximation is also employed in the present study. Since this study is concerned with essentially a viscous flow problem, however, a value of A is specified such that the second-order moment equations reduce to the Navier-Stokes shear stress-viscosity relationship near equilibrium. The present An is thus specified to be p/η, where $p = (\frac{1}{3})(p_s + p_n + p_b)$ and η is viscosity. The use of Holway's ellipsoidal statistical model[8] or the exact Maxwell-Boltzmann collision operator for Maxwell molecules (inverse fifth power repulsion) leads to the same result.

By setting Q equal to m, $m\xi_s$, $m\xi_n$, $m\xi_s{}^2$, $m\xi_n{}^2$, $m\xi_b{}^2$, and $m\xi_s\xi_n$, a set of seven first-order quasi-linear partial differential equations is obtained in terms of the seven flow parameters ρ,u,p_s,p_n,p_b,p_t and θ, where θ is the inclination of the streamline to the axis. These equations are listed as follows: when $Q = m$

$$(1/\rho)\,\partial\rho/\partial s + (1/u)\,\partial u/\partial s + \partial\theta/\partial n + \sin\theta/r = 0\quad(3)$$

when $Q = m\xi_s$

$$\frac{\partial p_s}{\partial s}+\frac{\partial p_t}{\partial n}+\rho u\frac{\partial u}{\partial s}-2p_t\frac{\partial\theta}{\partial s}+(p_s-p_n)\frac{\partial\theta}{\partial n}+\frac{\sin\theta}{r}(p_s-p_b)+\frac{\cos\theta}{r}p_t=0\quad(4)$$

when $Q = m\xi_n$

$$\frac{\partial p_n}{\partial n} + \frac{\partial p_t}{\partial s} + \rho u^2 \frac{\partial \theta}{\partial s} + 2p_t \frac{\partial \theta}{\partial n} + (p_s - p_n)\frac{\partial \theta}{\partial s} + \frac{\cos\theta}{r}(p_n - p_b) + \frac{\sin\theta}{r} p_t = 0 \quad (5)$$

when $Q = m\xi_s^2$

$$u\frac{\partial p_s}{\partial s} + 3p_s \frac{\partial u}{\partial s} + p_s u \frac{\partial \theta}{\partial n} + 2p_t \frac{\partial u}{\partial n} - 2p_t u \frac{\partial \theta}{\partial s} + \frac{\sin\theta}{r} u p_s - \frac{p}{\eta}(p - p_s) = 0 \quad (6)$$

$$\begin{bmatrix} \tau\frac{1}{\rho} & 0 & 0 & 0 & 0 & 0 \\ \tau\frac{1}{u} & \tau\rho u & 0 & \tau p_b & 3\tau p_s & \tau p_n \\ -1 & -(p_s - p_n) & \tau(\rho u^2 + p_s - p_n) & -p_b u & -p_s u & -3p_n u \\ 0 & \tau & 0 & 0 & \tau u & 0 \\ 0 & 0 & -1 & 0 & 0 & \tau u \\ 0 & 0 & 0 & \tau u & 0 & 0 \end{bmatrix} = 0 \quad (11)$$

when $Q = m\xi_n^2$

$$u\frac{\partial p_n}{\partial s} + p_n \frac{\partial u}{\partial s} + 3p_n u \frac{\partial \theta}{\partial n} + 4p_t u \frac{\partial \theta}{\partial s} + \frac{\sin\theta}{r} u p_n - \frac{p}{\eta}(p - p_n) = 0 \quad (7)$$

when $Q = m\xi_b^2$

$$u\frac{\partial p_b}{\partial s} + p_b \frac{\partial u}{\partial s} + p_b u \frac{\partial \theta}{\partial n} + 3\frac{\sin\theta}{r} u p_b - \frac{p}{\eta}(p - p_b) = 0 \quad (8)$$

when $Q = m\xi_s\xi_n$

$$u\frac{\partial p_t}{\partial s} + 2p_t \frac{\partial u}{\partial s} + 2p_t u \frac{\partial \theta}{\partial n} + (2p_s - p_n)u \frac{\partial \theta}{\partial s} + p_n \frac{\partial u}{\partial n} + \frac{\sin\theta}{r} u p_t + \frac{p}{\eta} p_t = 0 \quad (9)$$

These equations reduce to Edwards and Rogers' equations for constant u.

As with Edwards and Rogers, the set of moment equations was truncated by use of the hypersonic approximation. This approximation requires that the mass velocity u be much greater than a characteristic thermal velocity based on local temperature. This allows the consistent dropping of terms containing moments of higher order than the pressure and shear stress components.

In addition to the above equations, an energy equation may be obtained by setting $Q = (m/2)(\xi_s^2 + \xi_n^2 + \xi_b^2)$, or by simply adding the moment equations for $Q = m\xi_s^2$, $m\xi_n^2$, and $m\xi_b^2$. After some manipulations involving combinations with the moment equations for $Q = m$ and $m\xi_s$, the following is obtained:

$$\frac{\partial}{\partial s}\left(\frac{3p_s + p_n + p_b}{\rho} + u^2\right) + \frac{2}{\rho u}\left(\frac{\cos\theta}{r} - \frac{\partial \theta}{\partial s} + \frac{\partial}{\partial n}\right)(up_t) = 0 \quad (10)$$

For $p_t = 0$, the quantity $(3p_s + p_n + p_b)/\rho + u^2$ is seen to be conserved along streamlines. Although Eq. (10) is not used in the solution for the flowfield variables, it can be used as a check on the solution for $p_t = 0$.

Method-of-Characteristics Solution

The flowfield equations, Eqs. (3–9) developed in the preceding section form a hyperbolic set which may be solved numerically by the method of characteristics. For simplicity, p_t was set equal to zero, thus reducing the set of equations and variables from seven to six. The slope, $\tau = \tan\mu$, of the characteristic curve ζ with respect to the streamline s is found by solving the following determinant set equal to zero:

or

$$\tau = 0 \text{ and } \tau = \pm\left(\frac{3p_n + p_n^2/(\rho u^2 - 3p_s)}{\rho u^2 + p_s - p_n}\right)^{1/2} \quad (12)$$

An inspection of the above equation for $\tau \neq 0$ indicates that an imaginary slope would be obtained in some instances at Mach numbers near unity. The use of this analysis under those conditions, however, would be contradictory of the hypersonic approximation. The compatibility relations along the characteristic curve for $\tau = 0$ (along the streamline) are

$$\frac{\partial p_s}{\partial \zeta} + \frac{1}{u}(\rho u^2 - p_s + p_n)\frac{\partial u}{\partial \zeta} - \frac{(p_s - p_n)}{\rho}\frac{\partial \rho}{\partial \zeta} + \frac{\sin\theta}{r}(p_n - p_b) = 0 \quad (13)$$

$$\frac{\partial p_b}{\partial \zeta} - \frac{p_b}{\rho}\frac{\partial \rho}{\partial \zeta} + 2\frac{\sin\theta}{r} p_b - \frac{p}{u\eta}(p - p_b) = 0 \quad (14)$$

$$\frac{\partial p_s}{\partial \zeta} + 2\frac{p_s}{u}\frac{\partial u}{\partial \zeta} - \frac{p_s}{\rho}\frac{\partial \rho}{\partial \zeta} - \frac{p}{u\eta}(p - p_s) = 0 \quad (15)$$

$$\frac{\partial p_n}{\partial \zeta} - 2\frac{p_n}{u}\frac{\partial u}{\partial \zeta} - 3\frac{p_n}{\rho}\frac{\partial \rho}{\partial \zeta} - 2\frac{\sin\theta}{r} p_n - \frac{p}{u\eta}(p - p_n) = 0 \quad (16)$$

The compatibility relations for $\tau \neq 0$ are

$$\frac{\sin\mu}{p_n}[p_n^2 + (\rho u^2 - 3p_s)(\rho u^2 + p_s + 2p_n)]\frac{\partial \theta}{\partial \zeta} + \frac{\rho u^2 - 3p_s}{\cos\mu\ p_n}\frac{\partial p_n}{\partial \zeta} + \frac{\sin\theta}{r}(\rho u^2 - 3p_s + p_b) + \frac{\cos\theta\tan\mu}{r}(\rho u^2 - 3p_s)\frac{p_n - p_b}{p_n} - \frac{p}{u\eta}\left[p - p_s + (\rho u^2 - 3p_s)\frac{p - p_n}{p_n}\right] = 0 \quad (17)$$

Corner Expansion Equations

The usual finite difference method-of-characteristics equations cannot be applied directly to calculate the variation in

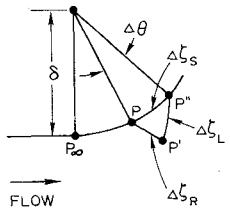

Fig. 1 Sketch of rounded-corner turn.

flow properties about a singular point such as a sharp-corner turn. It is necessary, therefore, to develop a special set of Prandtl-Meyer type relations for this purpose. Consider the rounded-corner turn shown in Fig. 1, where the streamline characteristic ζ_s follows the corner boundary, and ζ_R and ζ_L follow right and left-running characteristics. The solution of the corner expansion problem is obtained by using the method of characteristics to obtain the properties at the point P'' from the previously established properties at P and P', and then allowing δ and $\Delta\theta$ to approach zero. The streamline characteristic equations, Eqs. (13–16), become

$$\frac{dp_s}{d\theta} + (\rho u^2 - p_s + p_n)\frac{du}{ud\theta} - (p_s - p_n)\frac{d\rho}{\rho d\theta} = 0 \quad (18)$$

$$\frac{dp_b}{d\theta} - p_b\frac{d\rho}{\rho d\theta} = 0 \quad (19)$$

$$\frac{dp_s}{d\theta} + 2p_s\frac{du}{ud\theta} - p_s\frac{d\rho}{\rho d\theta} = 0 \quad (20)$$

$$\frac{dp_n}{d\theta} - 2p_n\frac{du}{ud\theta} - 3p_n\frac{d\rho}{\rho d\theta} = 0 \quad (21)$$

Equations (19–21) can be integrated as follows:

$$p_b/p_\infty = \rho/\rho_\infty \quad (22)$$

$$p_s/p_\infty = (\rho/\rho_\infty)/(u/u_\infty)^2 \quad (23)$$

$$p_n/p_\infty = (u/u_\infty)^2(\rho/\rho_\infty)^3 \quad (24)$$

where the ∞ subscript refers to conditions immediately prior to turning the corner. The following expression for u can be obtained by combining Eqs. (18, 20, and 24), neglecting terms of $p/\rho u^2$ compared to unity, and integrating:

$$u/u_\infty = \exp\{[3/(10M_\infty^2)][1 - (\rho/\rho_\infty)^2]\} \quad (25)$$

where

$$M_\infty^2 = (\tfrac{3}{5})(\rho_\infty u_\infty^2/p_\infty)$$

Applying Eq. (25) to Eqs. (22–24) results in four equations defining p_s,p_n, p_b and u in terms of ρ. This provides four of the five required equations for finding p_s,p_n,p_b,u and ρ in terms of θ. The fifth equation is obtained from the left-running characteristic equation and the variation of properties along $\Delta\zeta_L$.

$$\frac{dp_n}{\rho u^2} = -\sin\mu\cos\mu \times \frac{(p_n/\rho u^2)^2 + (1 - 3p_s/\rho u^2)[1 + (p_s + 2p_n)/\rho u^2]}{(1 - 3p_s/\rho u^2)}d\theta \quad (26)$$

Again neglecting terms of $p/\rho u^2$ compared to unity, using the approximation $\tan\mu \cong (3p_n/\rho u^2)^{1/2}$ and integrating yields:

$$\theta = \theta_\infty + [3/(5^{1/2}M_\infty)][1 - (\rho/\rho_\infty)] \quad (27)$$

Equations (22–25 and 27) are the five equations required for finding the variation of p_s,p_n,p_b, ρ and u with respect to θ. These equations, as mentioned previously, were obtained from characteristic equations which were, in turn, obtained from a set of partial differential equations in which the assumptions were made that the shear stress and all higher moments (heat flux, etc.) were negligible. These assumptions cannot be expected to be as accurate in the singular region about a sharp-corner turn as one would expect them to be in the mainstream. Nevertheless, the derived equations do provide a means of negotiating the corner turn, and any calculated flow peculiarities in the immediate vicinity of the sharp corner will be overridden by the mainstream flow after a few relaxation distances downstream of the corner. Moreover, in a real nozzle, a perfectly sharp corner does not exist, and, in addition, a boundary layer would be present to further round the flow about the corner.

Numerical Solution

The characteristics equations, Eqs. (13–17), were placed in finite difference form and programmed for a numerical solution on a digital computer. The corner expansion equations, Eqs. (22–25 and 27) were used to calculate the variation in flow properties around the nozzle lip. To insure stability in the numerical solution, the step size along the streamline characteristic must be less than the relaxation distance $u\eta/p$.

Discussion of Results

Before applying the calculation procedure developed in the preceding sections to a nozzle expansion, the accuracy of the technique was checked by application to the spherical source flow expansion investigated by Hamel and Willis.[1] The computer program was modified for calculating along a single ray running at a 45° angle to the axis. Spherical symmetry was imposed with the ray being a streamline. The properties at the starting location were taken from a continuum solution for spherical flow. Several different calculations were made in which the starting location and the step size were varied. It was found that so long as the step size was maintained smaller than that required for stability, the influence of step size on accuracy was negligible. The choice of starting location, however, was found to be considerably more important. The starting location must be chosen such that the flow is still near thermodynamic equilibrium. If this is not done, the calculated properties will initially lag behind the actual properties, and due to the rapid pace of the expansion process coupled with the continual decrease in magnitude of the relaxation terms, the calculated values will be unable to overtake the actual values. Shown in Fig. 2 are the method-of-characteristics calculated temperatures, T_s and T_n, compared with the calculations of Hamel and Willis. The source Reynolds number is given here in terms of an inverse source Knudsen number Kn_D^{-1}, of

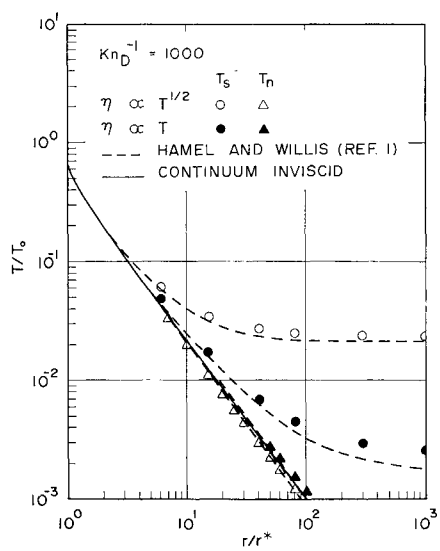

Fig. 2 Temperature variation for spherical source flow.

1000 based on an equivalent freejet orifice diameter (see Hamel and Willis). For hard sphere molecules ($\eta \propto T^{1/2}$), the present results for both T_s and T_n are seen to compare very closely with Hamel and Willis. Fair agreement is obtained for Maxwell molecules ($\eta \propto T$).

After establishing at least a reasonable degree of accuracy for the analytical technique, the method was applied to a nozzle expansion with uniform parallel flow at the exit with no boundary layer. There is no problem in this case with the starting values, as was encountered with spherical flow, because the uniform parallel flow initial conditions require that the pressure components be initially equal. Figure 3 is a plot of density contours for throat Reynolds numbers Re^* of 25 and 100 compared to continuum inviscid flow. The continuum inviscid calculations were made using the computer program described in Ref. 9. The two rarefied flow cases are seen to compare very closely with the continuum inviscid case. Slight differences are noted near the high curvature points on the contours. These small differences, however, may be due to the errors in the numerical calculations being accentuated in this high curvature region. Also, the corner expansion equation may introduce small errors which are propagated outward in this fashion. It was mentioned previously in the derivation of the corner expansion equations that the assumptions of zero shear stress and heat flux could not be considered very accurate in the neighborhood of a sharp corner turn.

Another perspective of the density variation is seen in the axial distribution shown in Fig. 4 and in the radial distribution shown in Fig. 5. In Fig. 4 both the rarefied flow cases and the continuum inviscid case are compared to a faired straight line of slope equal to -2. Both the rarefied flow cases and the continuum inviscid case should approach a straight line of this slope in the outer limit. Close agreement is observed between the rarefied flow cases and the continuum inviscid case, and both are seen to lie very close to the faired line. The radial distribution in Fig. 5 is shown out to the outer limit of the calculations. Fairly close agreement is again shown in the rarefied flow cases and the continuum inviscid case.

The axial temperature distribution, for both T_s and T_n, is shown in Fig. 6. On the axis, T_b is identical to T_n. T_s is seen to depart from continuum inviscid flow and approach a constant as the distance is increased. T_n, however, remains very close to continuum inviscid. The radial temperature distribution for T_s, T_n and T_b is shown in Fig. 7. At this axial location, T_s has already departed significantly

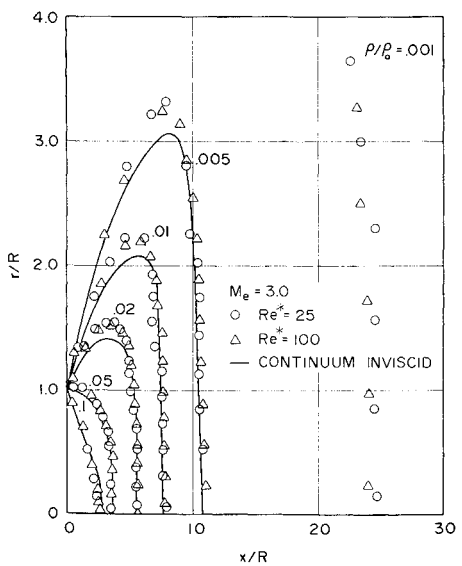

Fig. 3 Density contours for rarefied flow compared to continuum inviscid flow.

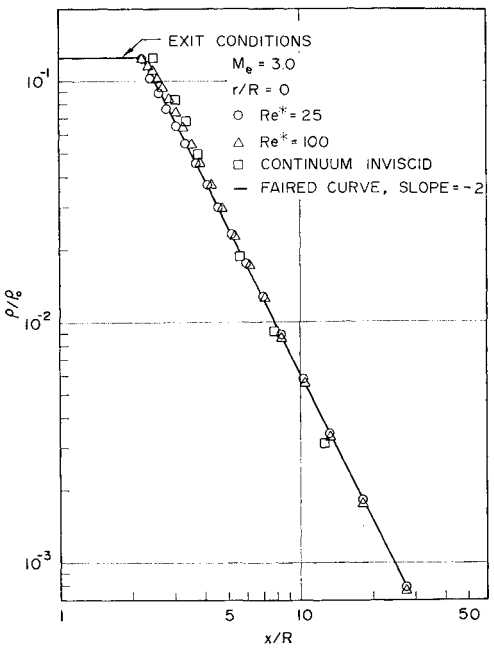

Fig. 4 Axial density distribution for rarefied flow compared to continuum inviscid flow.

from continuum inviscid flow on the axis (Fig. 6). As the radial position is increased, T_s remains relatively constant. T_n and T_b are identical on the axis, and, as r/R increases, T_n decreases continuously, with T_b lagging somewhat behind.

Conclusions

These results indicate that noncontinuum flow effects do not have a very large influence on the density and velocity fields for nozzles of throat Reynolds numbers down to at least 25. This is true even out in the far field where extremely low densities are encountered. For high Reynolds number nozzles, where noncontinuum effects do not become manifest until the flow is hypersonic (velocity is nearly at the thermodynamic limit and the streamlines are nearly straight), the density field downstream is determined solely by the geometrical divergence of the straight streamlines.

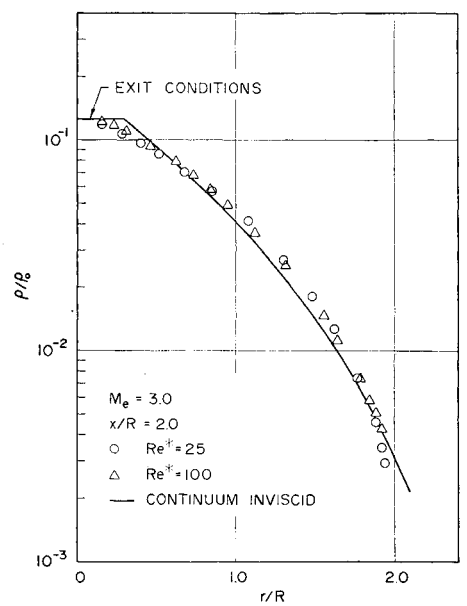

Fig. 5 Radial density distribution for rarefied flow compared to continuum inviscid flow.

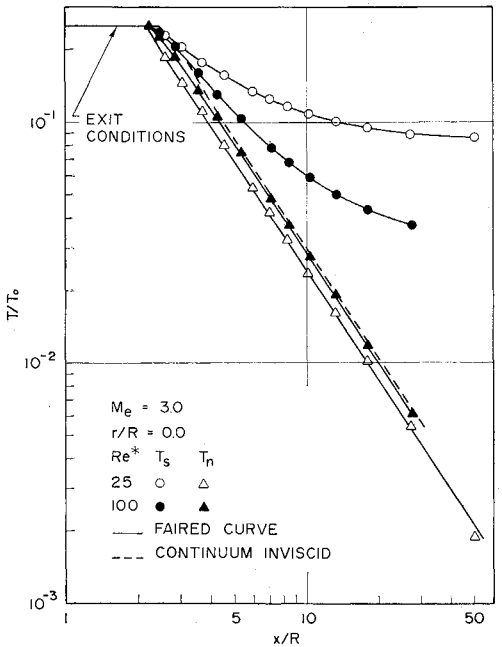

Fig. 6 Axial temperature distribution for rarefied flow compared to continuum inviscid flow.

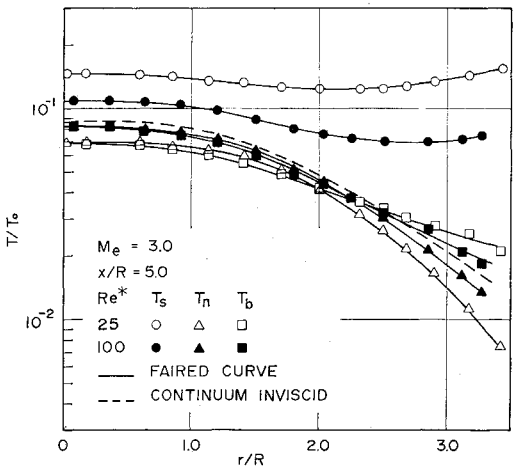

Fig. 7 Radial temperature distribution for rarefied flow compared to continuum inviscid flow.

The density field, therefore, is essentially unaffected by transition from continuum flow. Even for the very low Reynolds number nozzles investigated herein, the density field does not appear to be affected significantly by transition to noncontinuum flow.

The temperatures were found to display noncontinuum effects in much the same fashion as predicted previously for spherical source flow; i.e., the parallel component T_s approaches a limiting finite value while the perpendicular components T_n and T_b continue to approach zero. For the usual high Reynolds number jet exhausting into a vacuum, however, these effects occur at very low values of temperature, and, therefore, have little effect on the energy content and flow of the gas.

The above results indicate that it may be possible to calculate fairly accurate flowfield temperatures by calculating an effective source density for each streamline, and then computing the temperature along the streamline by using the theory of Ref. 1.

The authors' attention has recently been directed to the "jet shredding" effect discussed in Ref. 10. This effect is the disruption of streamlines due to transverse thermal streaming. Although jet shredding was not investigated specifically in the present study, the analytical technique described herein would appear to be useful in the investigation of this effect.

References

[1] Hamel, B. B. and Willis, D. R., "Kinetic Theory of Source Flow Expansion with Application to the Free Jet," *The Physics of Fluids*, Vol. 9, 1966, p. 829.

[2] Edwards, R. H. and Cheng, H. K., "Steady Expansion of a Gas into a Vacuum," *AIAA Journal*, Vol. 4, No. 3, March 1966, p. 558.

[3] Willis, D. R. and Hamel, B. B., "Non-Equilibrium Effects in Spherical Expansions of Polyatomic Gases and Gas Mixtures," *Rarefied Gas Dynamics* edited by C. L. Brundin, Vol. I, Academic Press, New York, 1967, p. 837.

[4] Edwards, R. H. and Rogers, A. W., "Steady Non-Isentropic Jet Expansion into a Vacuum," AIAA Paper 66-490, Los Angeles, Calif., 1966.

[5] Peracchio, A. A., "Kinetic Theory Analysis for the Flow Field of a Two-Dimensional Nozzle Exhausting to Vacuum," AIAA Paper 69-658, San Francisco, Calif., 1969.

[6] Robertson, S. J., "Method-of-Characteristics Solution of Rarefied Monatomic Gaseous Jet Flow into a Vacuum," LMSC/HREC D148961, Aug. 1969, Lockheed Missiles & Space Co., Huntsville, Ala.

[7] Bhatnagar, P. L., Gross, E. P., and Krook, M., "A Model for Collision Processes in Gases. I. Small Amplitude Processes in Charged and Neutral One-Component Systems," *Physics of Fluids*, Vol. 94, 1954, p. 511.

[8] Holway, L. H., "Kinetic Theory of Shock Structure Using an Ellipsoidal Distribution Function," *Rarefied Gas Dynamics* edited by J. H. deLeeuw, Vol. I, Academic Press, New York, 1965, p. 193.

[9] Prozan, R. J., "Development of a Method-of-Characteristics Solution for Supersonic Flow of an Ideal, Frozen or Equilibrium Reacting Gas Mixture," LMSC/HREC A782535-A, April 1966, Lockheed Missiles & Space Co., Huntsville, Ala.

[10] Muntz, E. P., Hamel, B. B., and Maguire, B. L., "Exhaust Plume Rarefaction," AIAA Paper 69-657, San Francisco, Calif., 1969.